Separation Science and Technology
Publication details, including instructions for authors and subscription information:
http://www.informaworld.com/smpp/title~content=t713708471

NANOLEVEL MAGNETIC SEPARATION MODEL CONSIDERING FLOW LIMITATIONS

Gregory B. Cotten[a]; H. Bradley Eldredge[b]
[a] Department of Chemistry, United States Naval Academy, Annapolis, MD, U.S.A. [b] Eldredge Engineering, Idaho Falls, ID, U.S.A.

Online publication date: 12 February 2002

To cite this Article Cotten, Gregory B. and Eldredge, H. Bradley(2002) 'NANOLEVEL MAGNETIC SEPARATION MODEL CONSIDERING FLOW LIMITATIONS', Separation Science and Technology, 37: 16, 3755 — 3779
To link to this Article: DOI: 10.1081/SS-120014830
URL: http://dx.doi.org/10.1081/SS-120014830

MARCEL DEKKER, INC. • 270 MADISON AVENUE • NEW YORK, NY 10016

SEPARATION SCIENCE AND TECHNOLOGY
Vol. 37, No. 16, pp. 3755–3779, 2002

NANOLEVEL MAGNETIC SEPARATION MODEL CONSIDERING FLOW LIMITATIONS

Gregory B. Cotten[1,*] and H. Bradley Eldredge[2]

[1]Department of Chemistry, United States Naval Academy,
572 Holloway Rd, Annapolis, MD 21402
[2]Eldredge Engineering, 1111 Caysie Ln,
Idaho Falls, ID 83402

ABSTRACT

This work proposes an enhanced nanolevel magnetic separation model considering flow limitations using simplifying assumptions. The theoretical model builds on magnetic heteroflocculation models described in the literature and couples the magnetic and hydrodynamic forces between two spherical particles with different sizes and different magnetic properties under bulk fluid flow conditions. Separator performance figures are presented showing the relationship between input parameters such as applied magnetic field strength, flow rate, and matrix material size and composition, and output parameters such as Peclet number and capture propensity for various contaminant particle sizes. This purely predictive model work may be useful in estimating actual

*Corresponding author. Fax: (410) 293-2218; E-mail: cotten@usna.edu

DOI: 10.1081/SS-120014830
0149-6395 (Print); 1520-5754 (Online)

magnetic separator performance and serve as a starting point for experimental work or more accurate mathematical models.

This work provides a simplified mathematical model to predict magnetic separator performance based on single magnetic matrix particle and single magnetic contaminant particle interactions. Local maxima, or transition points, between matrix and contaminant particle size and separator performance indicate magnetic separator performance can be optimized by the selection of appropriate magnetic matrix particle size. Evaluation of points of maximum particle capture force using the Peclet number provides limiting conditions for retention of particles under Stokes flow conditions.

Key Words: Magnetic separation; Modeling; Particle; Hydrodynamics; Magnetite

INTRODUCTION

Magnetic separations are widely used in many industries including minerals separation,[1] municipal and industrial wastewater treatment,[2] and plutonium inventory and accountability.[3] Recent improvements in electromagnet designs and associated lower capital and operating costs make magnetic separations more feasible today than ever.[4] One class of magnetic separations, commonly called high gradient magnetic separation (HGMS), relies on high magnetic field gradients being established in and around the magnetic matrix material to affect particle capture. This has been achieved with high external applied magnetic field strengths on the order of 2–10 T and fine stainless steel wool mesh being used as the magnetic matrix material.[5–7]

Commercial scale magnetic separators operate on gross scale performance with throughputs in tons per hour. In general, magnetic separation theory has focused on single contaminant particle–single magnetic matrix interaction.[8] The extrapolation from theoretical particle–matrix performance curves to industrial scale application involves a quantum jump in complexity as the inter-matrix and inter-particle force relationships result in, as of yet, intractable solutions. Real-world applications are more difficult to model due to magnetic field distribution and interaction complexities. In addition, the buildup of particles on magnetic matrices results in diminished removal efficiency.[9] These scale-up problems have been overcome in the industrial applications by conservative designs, recycle streams, and careful monitoring of process variables.[10,11]

Recent microscopic-scale theory and application of magnetic separators approach the problems associated with separation of nonfilterable

nanoparticles[12–19] and nuclear material nonproliferation control.[20–22] These processes, characterized as low throughput with typically dilute contaminant concentrations, are more easily modeled using numerical simulations because many of the necessary simplifying assumption are generally applicable. This work builds on the theoretical models existing in the literature and couples a hydrodynamic flow component to previous magnetic attractive force theory where only Brownian motion was considered. Magnetic separator performance under various conditions is evaluated.

THEORY AND MODEL DEVELOPMENT

Nomenclature

B	Magnetic induction (T, Wb m^{-2})
dB/dz	Magnetic field induction gradient
F_d	Hydrodynamic drag force (N)
F_m	Magnetic force (N)
H	Magnetic intensity (A m^{-1})
k	Boltzmann's constant [1.38×10^{-23} (J K^{-1})]
M_I	Induced magnetic field intensity (A m^{-1})
$M_{I,s}$	Induced magnetic field intensity at saturation (A m^{-1})
P_c	Contaminant particle
Pe	Peclet Number, defined by Eq. (7)
r	Radial distance between particles (m)
Re_p	Particle Reynolds number (dimensionless), defined by Eq. (9)
r_p	Particle radius (m)
r_c	Contaminant particle radius (m)
r_m	Matrix particle radius (m)
T	Temperature (K)
V	Particle volume (m^3)
ϑ	Magnetic separator performance factor (dimensionless), defined by Eq. (10)
ρ	Fluid density (kg m^{-3})
θ	Angle in spherical coordinate system as depicted in Fig. 1
μ	Fluid viscosity (Pa sec), used in Eq. (1)
μ_m	Magnetic permeability of the medium [Wb(A m)$^{-1}$], used in Eq. (A1)
$\mu_{p,m}$	Magnetic permeability of the matrix particle [Wb(A m)$^{-1}$], used in Eq. (A3)
μ_0	Magnetic permeability of free space [$4\pi \times 10^{-7}$ Wb(A m)$^{-1}$], used in Eq. (4)

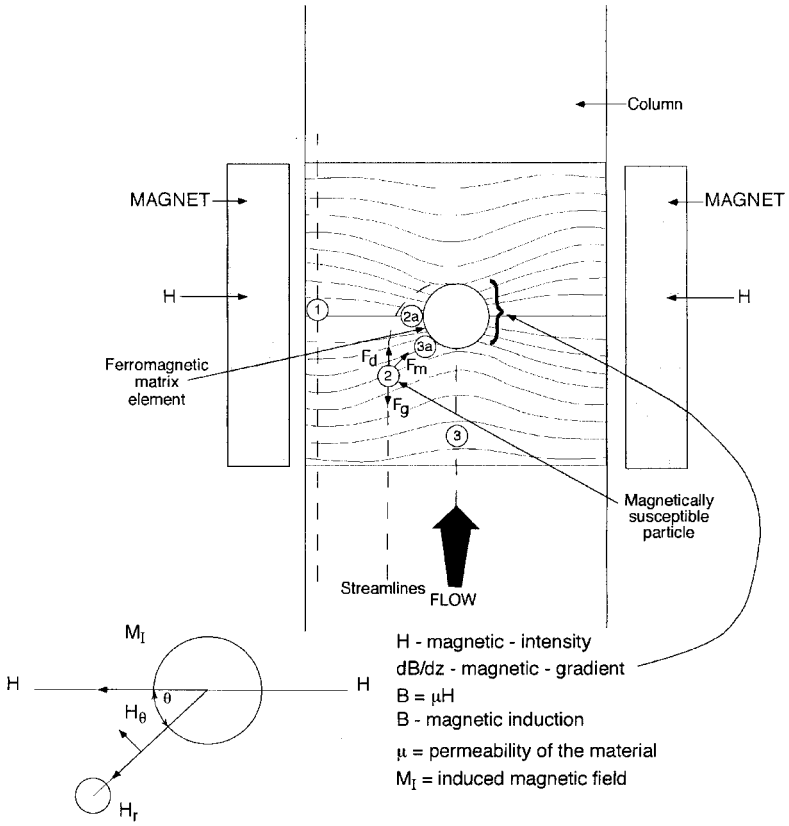

Figure 1. Representation of a magnetic separator employing a magnetite particle as the magnetic matrix (adapted from Ref. [38]).

ν	Fluid velocity ($\mathrm{m\,sec^{-1}}$)
χ	Magnetic susceptibility (dimensionless)
χ_c	Magnetic susceptibility of the contaminant particle (Table 1)
χ_m	Magnetic susceptibility of the medium, water (-1.3×10^{-6})

There is a substantial amount of literature regarding single wire element magnetic separation of nanoparticles including both theoretical and experimental presentations.[23–26] In addition, flocculation studies have been performed in support of magnetic seeding theory.[27–32] To date, the development of theoretical models that couple a spherical magnetic matrix material and single particle interaction under the influence of forces other than Brownian motion are limited.[33–35] In contrast to theoretical prediction of electric field-enhanced

Table 1. Magnetic Susceptibility (χ) of Particles Shown in Fig. 3

Compound	Value (Dimensionless)
$FeCl_2$	$14{,}750 \times 10^{-6}$
$CoCl_2$	$12{,}660 \times 10^{-6}$
$Fe(OH)_2$	$12{,}000 \times 10^{-6}$
UCl_4	$3{,}680 \times 10^{-6}$
UCl_3	$3{,}460 \times 10^{-6}$
PuO_2	730×10^{-6}
$CaCl_2$	-54.7×10^{-6}
$MgCl_2$	-47.4×10^{-6}

coalescence of spherical drops[36] and hydrodynamic diffusion of suspended particles,[37] this work evaluates particle–particle interaction under magnetic attraction and Stokes flow conditions using nanometer-size particles. It is desirable to evaluate magnetic separations employing spherical magnetic matrix material to expand this limited body of knowledge and more accurately reflect performance of real magnetic separation devices. Although work by Ebner et al.[19] have evaluated polymer spheres constructed with interstitial magnetite, this work evaluates simply using pure magnetite as the magnetic matrix. Small magnetic matrix particles offer several advantages over stainless steel wire mesh. Magnetite particles are ubiquitous in nature making them available and inexpensive. Small particles offer a higher degree of magnetic gradient curvature: this is one of the major costs associated with wire systems where the geometry is typically altered to increase magnetic curvature. The wire cross-sections are altered through geometrically complex extrusion or the growth of dendrites on common wire to increase the angularity of the matrix material and to thus increase magnetic curvature, or the bending of the magnetic lines of flux. The high magnetic gradients offer improved magnetic separation efficiency.

Figure 1 depicts an idealized treatment column for magnetic separation where three idealized magnetically susceptible particles are shown to encounter a single magnetic matrix element (adapted from Ref. [38]). The magnetic matrix element here is a roughly spherical magnetite ($FeO{\cdot}Fe_2O_3$) particle, which is the column packing material for this work. For these studies, the arbitrary magnetically susceptible contaminant particles can interact with the column in one of three ways. Particle #1 has a flow streamline that carries it through the column without interaction with the matrix element due to a combination of two principles. The hydrodynamic drag force is given by Stokes' law

$$|\vec{F}_d| = 6\pi r_p \mu \nu \tag{1}$$

and the magnetic force is given by

$$|\vec{F}_{\mathrm{m}}| = \chi HV \frac{\mathrm{d}B}{\mathrm{d}z} \tag{2}$$

Other forces do exist such as inertial, gravitational, and buoyant, but are neglected in these discussions as the assumption of very small contaminant particle size is being employed.

The magnetic matrix element will have an induced magnetic attractive force to the contaminant particle and the contaminant particle will have an induced magnetic moment while in the influence of both the external magnetic field and the induced field in the magnetic matrix. For magnetic separation to occur, the necessary, but not sufficient condition is

$$|\vec{F}_{\mathrm{m}}| \geq |\vec{F}_{\mathrm{d}}| \tag{3}$$

The magnetic force must overcome the drag force for magnetic separation to occur when the particles are touching. If the hydrodynamic drag force exceeds the magnetic force, the particle will be swept away in the bulk fluid. The magnetic and drag forces have vector components as shown in Fig. 1. The resulting vector sum between the magnetic and drag forces will be a function of the relative position of the particles and their angular deflection from the normal component of the external magnetic field and the bulk fluid streamlines. It is assumed here that the particle traveling with the bulk velocity does not have any drag force since there is no relative velocity between the bulk fluid and the particle (i.e., no slip due to small particle size). When a magnetic attractive force interacts with the particle, it can deviate from the streamline and this induces a change in the trajectory and relative velocity of the particle. The drag force steadily increases as the particle velocity slows from the bulk velocity until it reaches a maximum at particle capture. For particle #1 in Fig. 1, the magnetic force is insufficient to change the particle's trajectory from the streamline. Since the particles never touch, Eq. (3) is not satisfied and the bulk fluid flow carries the particle through the column.

The path taken by particle #2 depicts the "capture radius*" concept whereby the contaminant particle and matrix particle magnetic forces are such that given the distance between the particles, Eq. (3) is satisfied and capture, via magnetic separation, has occurred (see particle #2a).

*The capture radius is the maximum distance between the contaminant particle and the streamline that goes through the center of the magnetic matrix particle by which retention is achieved.

The particle depicted as #3 is in a streamline whereby a collision course is predetermined regardless of magnetic attraction. Magnetic forces can alter the collision path due to the orthogonal relationship between the applied magnetic field intensity and the particle matrix orientation (see "Results and Discussion"), but depending on the conditions, magnetic separation may occur as shown by particle #3a.

The development of a hydrodynamic drag force and magnetic force relationship, which can be solved for the variables of interest, is as follows. These variables can be grouped into dimensionless quantities such as the particle Reynolds or Peclet numbers. Ebner et al.[39] starts with the expression of the magnetic force exerted by the magnetic matrix particle on the contaminant particle as

$$\vec{F}_{\mathrm{m}} = \frac{2}{3}\pi r_{\mathrm{c}}^3 \mu_0 (\chi_{\mathrm{c}} - \chi_{\mathrm{m}}) \nabla (H^2) \tag{4}$$

and for the specific case, where particle–particle attraction is to be evaluated in a uniform external applied magnetic field and under the assumption of spherical particles, the radial and angular components of the magnetic force modified from Ref. [39] are

$$\vec{F}_{\mathrm{m_{radial}}} = \left[-\frac{4}{3}\pi r_{\mathrm{c}}^3 \mu_0 (\chi_{\mathrm{c}} - \chi_{\mathrm{m}}) \left(\frac{r_{\mathrm{m}}^3 M_{\mathrm{I}}}{r^4} \right) \left[2\left(H + \frac{2r_{\mathrm{m}}^3}{3r^3} M_{\mathrm{I}} \right) \cos^2\theta + \left(-H + \frac{r_{\mathrm{m}}^3}{3r^3} M_{\mathrm{I}} \right) \sin^2\theta \right] \right] e_r \tag{5}$$

$$\vec{F}_{\mathrm{m_{angular}}} = \left[\frac{4}{3}\pi r_{\mathrm{c}}^3 \mu_0 (\chi_{\mathrm{c}} - \chi_{\mathrm{m}}) \left[-\left(H + \frac{2r_{\mathrm{m}}^3}{3r^3} M_{\mathrm{I}} \right)^2 + \left(-H + \frac{r_{\mathrm{m}}^3}{3r^3} M_{\mathrm{I}} \right)^2 \right] \frac{\cos\theta \sin\theta}{r} \right] e_\theta \tag{6}$$

where r and θ are the radial and angular components of the separation between the matrix particle and the contaminant particle (see Fig. 1). By inspection of Eqs. (5) and (6), it is apparent that the magnetic attractive force is maximized when $\theta = 0°$. The angular component tends to move the contaminant around the matrix particle to this ultimate position.

Ebner et al.[39] developed equations similar to Eqs. (5) and (6) and applied them to Brownian motion forces using a variant of the Peclet number as shown by

$$Pe = \frac{r_{\mathrm{c}} |\vec{F}_{\mathrm{m}}|}{kT} \tag{7}$$

where the dimensionless Peclet number indicates that the magnetic force dominates when $Pe \gg 1$. We have chosen $Pe \geq 10$ as the conservative criteria for magnetic forces to dominate over Brownian forces.

The model developed by Ebner et al.[39] did not consider the hydrodynamic forces associated with a particle in a flowing stream; therefore the emphasis of this work is to expand upon this earlier model to describe limiting criteria or maximum expected performance and to include hydrodynamic flow forces due to bulk fluid velocity.

Combining Eqs. (3), (5), and (6) yields the following equation combining magnetic forces and flow forces which must be satisfied for magnetic separation to occur.

$$|\vec{F}_{\mathrm{m_{radial}}} + \vec{F}_{\mathrm{m_{angular}}}| \geq 6\pi r_{\mathrm{c}} \mu \nu \tag{8}$$

We now have added the drag force to the model and since the magnetite matrix particles are ferromagnetic, their magnetic force is much greater than the drag force and hence they remain in the bed. As Stokes law is only applicable under specific flow conditions,[40] a dimensionless number is typically used to evaluate these conditions. The particle Reynolds number,

$$Re_{\mathrm{p}} = \frac{2 r_{\mathrm{p}} \nu \rho}{\mu} \tag{9}$$

should be less than 0.1 for Stokes law to be valid for describing the hydrodynamic drag on a particle. Since this work is limited to nanoparticles in Stokes flow conditions, plots of separator performance in terms of particle Reynold's number are provided (see "Results and Discussion").

The magnetic force and hydrodynamic force are related through the introduction of an arbitrary dimensionless variable representing the magnetic separator performance factor

$$\vartheta = \frac{|\vec{F}_{\mathrm{m}}|}{|\vec{F}_{\mathrm{d}}|} \tag{10}$$

where magnetic forces dominates when $\vartheta > 1$. Referring to Fig. 1, the radial component of the magnetic force, as shown in Eq. (5), is maximized when the contaminant particle is in line with the applied magnetic field intensity and the matrix particle, where $\theta = 0^\circ$. The drag force is assumed to be purely in the z direction although in an actual packed bed column, streamlines would vary in direction consistent with column porosity and flow past matrix material. The magnetic force varies with θ, which would typically start out at near 90° for the particle expected to pass within the capture radius and decrease to near 0 at capture. The angular component of the magnetic force will tend to force the particle into this position and at 90°, the radial component is maximized

in repulsion. However, at $\theta = 0°$ and considering the particles as point sources, the magnetic force and drag force are orthogonal. Assuming surface friction is minimal, the drag force will cause the particle to move out of the $\theta = 0$ position at which point the radial and angular components of the magnetic force will develop z direction components.

RESULTS AND DISCUSSION

Equations (5)–(10) were entered into a declarative, rule-based programming package, TK Solver (Version 3.32, Universal Technical Systems, Inc., Rockford, IL) where the equations were solved for the various outputs to be presented. The software package allows for the direct entry of all known equations in standard form, without the need to perform any algebraic manipulation to solve for the dependent variables.

Magnetite was selected not only on a cost and abundance basis, but also since magnetite particles are roughly spherical and antiferromagnetic; they exhibit a behavior similar to ferromagnets but with reduced strength due to the antiparallel arrangement of the coupled spins. Therefore, magnetite has high magnetization and very low hysteresis, which would facilitate contaminant particle release and separation with the removal of the external magnetic field.[39]

Magnetite develops a magnetic saturation, $\mu_0 M_{I,s}$, where an increase in applied magnetic field intensity does not increase the magnetic induction, of 0.615 T in an applied field, $\mu_0 H$, of 2.15 T.[41,42] This is consistent with values used by Ebner et al.,[39] which were $\mu_0 M_{I,s} = 0.6\,\mathrm{T}$ and $\mu_0 H = 2\,\mathrm{T}$, respectively.

Figure 2 is a reproduction of Fig. 6 from Ref. [39] with the corrected values applied.* The separation distance, r, is arbitrarily set by Ebner et al.[39] at three times the matrix particle radius.

The magnetic force is maximized when the contaminant particle is touching, where

$$r_{min} = r_c + r_m \tag{11}$$

*Some clarification is required to the values reported in Ref. [39]. Applied magnetic field values reported in their figures are erroneously reported as "$H_a = \mathrm{X.X\,T}$" where the units are incorrect. One must either divide by μ_0 to obtain the correct value in $\mathrm{A\,m^{-1}}$ or represent the quantity as $\mu_0 H$, as is done in this work. The output values represented in their figures are off by a factor of one half. The magnetite magnetic saturation value reported as "$M_{s,m} = 4.8 \times 10^{-5}\,\mathrm{A\,m^{-1}}$" includes a typographical error on the sign of the exponent. These items have been confirmed with Ebner through personal correspondence.

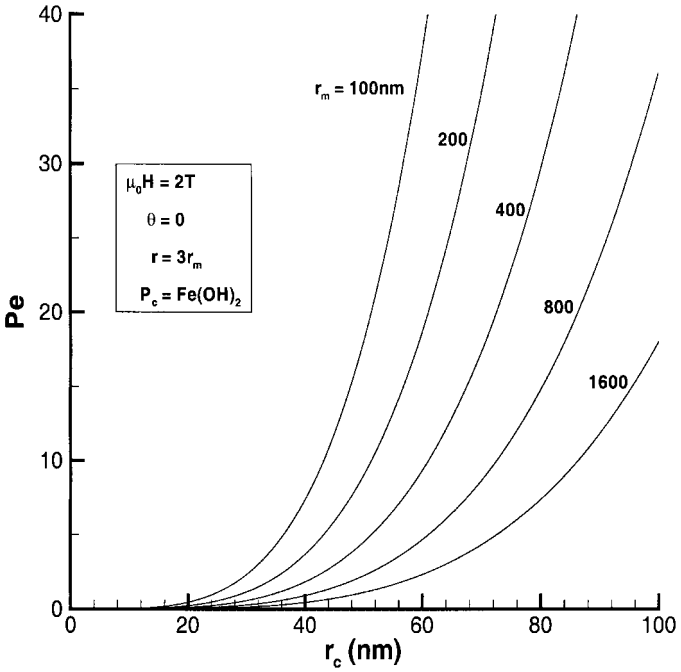

Figure 2. *Pe* as a function of r_c with different r_m (corrected from Fig. 6 of Ref. [39]).

and the matrix particle is aligned linearly with the applied magnetic field intensity where $\theta = 0^\circ$ and the angular component of the magnetic force is 0. Any condition deviating from these would only tend to reduce the potential for effective magnetic separation. In addition, these conditions represent the maximum drag force as the particle will encounter the full unaltered bulk fluid flow. If magnetic separation is not possible under these conditions, it is unlikely that magnetic separation will work at all. In other words, this is a "best case" scenario used for limiting process variables.

Figure 3 compares the corrected results obtained by Ebner et al.[39] with several other contaminants in a variety of particle size, but identical input conditions (as Fig. 2) except for the matrix particle size and separation distance. Larger magnetite matrix particles of 1000 nm radius were used as this size more accurately represents the commercially available material. The Peclet number represents the magnitude of magnetic force compared to Brownian force, with the magnetic forces dominating when $Pe \geq 10$. Figure 3 represents a stagnant magnetic separator where there are no flow forces. The utility of this figure lies in the visualization of the hierarchy of potential contaminant separation for

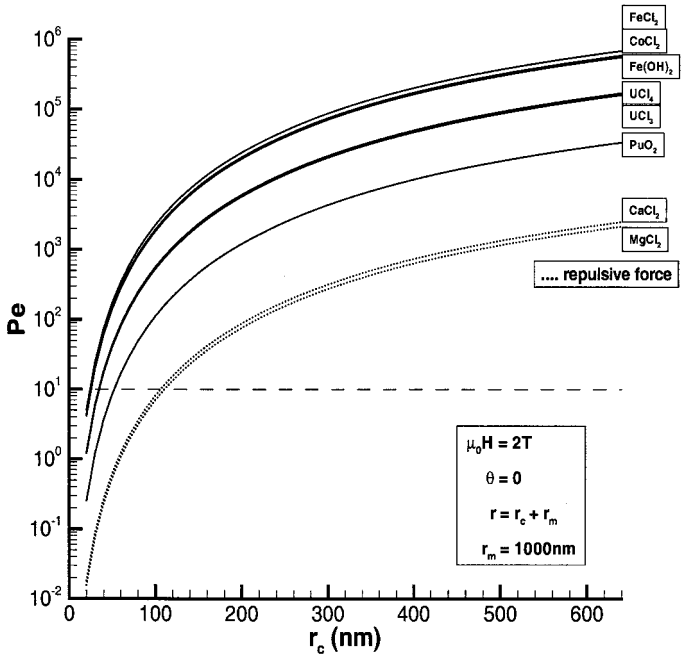

Figure 3. *Pe* as a function of r_c with different contaminant particles at r_{min}.

the various species whose magnetic susceptibilities are shown in Table 1. In addition, note that substantial decrease in the relative value of the magnetic force in relation to the Brownian force as the particle size decreases. The diamagnetic particles, $CaCl_2$ and $MgCl_2$, have repulsive forces although they appear to be attractive on Fig. 3. This is due to the treatment of the force in Eq. (7) where the sign of the magnetic force is lost. The diamagnetics indeed do have a repulsive force to the magnetic matrix element in this orientation and Fig. 3 shows this force to be small in comparison to other para- and ferro-magnetic particles. A dashed line is provided at $Pe = 10$ to indicate the threshold we established to indicate magnetic separation. Diamagnetic particles with radii less than approximately 100 nm would not be expected to be repulsed and paramagnetic and ferromagnetic particles with radii less than approximately 50 nm would not be expected to be magnetically separated.

Plutonium dioxide particles were selected for additional presentation in this work because they are weakly paramagnetic which helps to define the limits of this technology as contaminant particles with larger magnetic susceptibilities would be more easily magnetically separated. Plutonium dioxide is a component

of nuclear weapons, reactor, and nonproliferation systems where magnetic separation for water and waste treatment might be applied. Note that the use of discretely sized contaminant particle is for theoretical model purposes. Actual waste may or may not contain discrete size ranges or particles of this size.

Figure 4 shows the impact of matrix particle size and its associated magnetic gradient on contaminant particle capture as a function of contaminant particle size. In this model run, the contaminant particle is iron hydroxide, but the separation distance is set to r_{min} to maximize the magnetic attractive force. The curves have intersections at r_c equal to approximately 45, 85, 175, and 340 nm. These intersections represent transition points for magnetic separator performance and thus limiting conditions for matrix to contaminant particle radius ratios. The transitions occur where the contaminant particle radius ratio approaches a limiting value for the smaller r_m curve and transitions to approximately 0.25 or less for the larger r_m curve. The larger r_m curve shows improved magnetic separation performance as *Pe* is larger and increasing at an increasing rate compared to the smaller r_m curve.

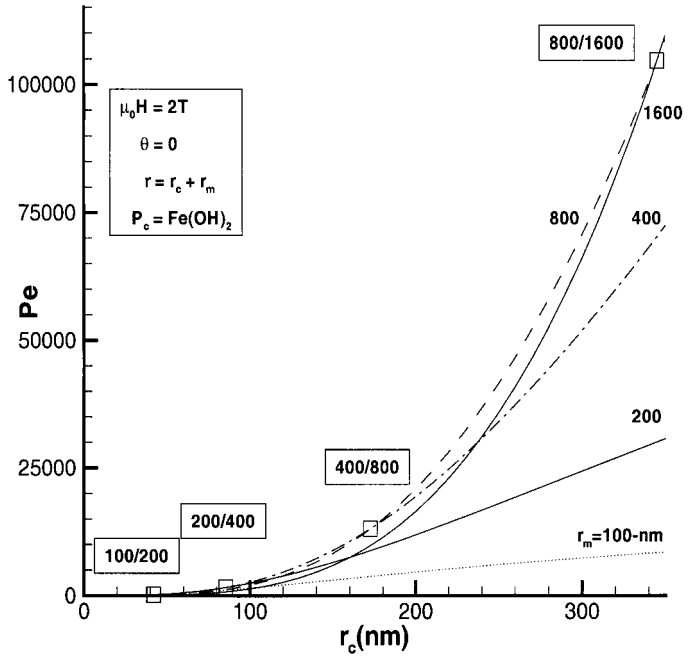

Figure 4. *Pe* as a function of r_c with different r_m at r_{min}.

This suggests that the high curvature of small matrix particles offers a benefit up to a limiting point (curve cross-over point) where the Brownian thermal diffusion force induced by the contaminant particle size becomes relatively more dominant over the magnetic attractive force. The theoretical model predicts that increasing matrix particle size can, therefore, improve magnetic separation for a given contaminant particle size at the identified transition points. This is essential to process optimization as it clearly suggests that magnetic matrix material can be optimized for discrete particle removal, if the contaminant particle size is well characterized.

It is important to evaluate model parameters using Ebner et al.[39] representation of the Peclet number expression prior to evaluating the flow component of this work. If a magnetic separator will not perform under Brownian motion external forces, then it surely will not function when hydrodynamic forces are added. Peak performance, as indicated by maximum Peclet values, provides a satisfactory starting point to understanding the limitations of a magnetite-based magnetic separator under flowing column applications.

Plutonium dioxide particles were evaluated based on their magnetic susceptibility and their importance in the nuclear weapons/fuel cycle. Figure 5 shows the minimum PuO_2 particle size that could be magnetically separated with magnetite as the magnetic matrix material under the stipulated magnetic field.

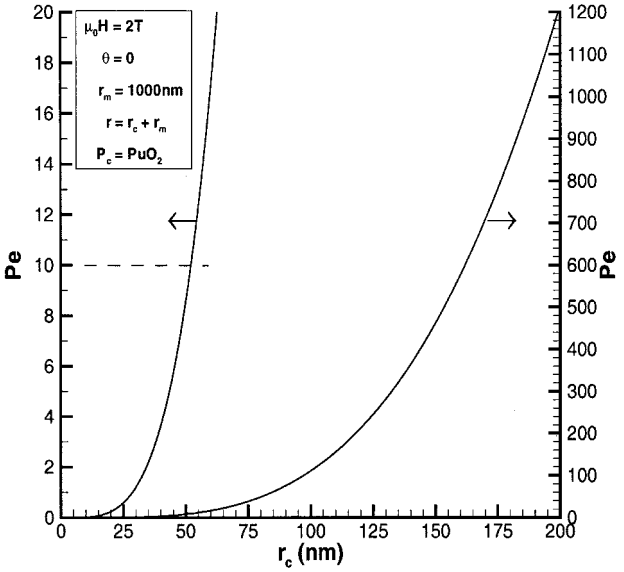

Figure 5. *Pe* as a function of r_c for $P_c = PuO_2$ at r_{min}.

Assuming $Pe \geq 10$ as the reference point for particle capture, a particle of 50 nm radius would be expected to be retained under external forces limited to Brownian motion. The two curves are actually the same data with different *Pe* axis to more clearly show the detail for r_c less than 50 nm. Note the arrows on the curves in Fig. 5 point to their respective Peclet axis. We will show later the effects of flow-induced drag.

Figure 6 expands on the transition points concepts observed in Fig. 4. If the magnetic matrix particle radius to the contaminant particle radius ratio can be controlled, theoretical magnetic separation efficiency can be maximized. Starting with the Peclet number maximized is the logical point to evaluate flow, since this represents the column conditions when flow is shut off. With the matrix particle size optimized to the contaminant particle size, flow conditions can be evaluated to determine the limiting conditions for particle capture and retention in a magnetic separator.

Figures 6–9 shows the optimum matrix and contaminant particle size combinations for $Fe(OH)_2$ and PuO_2. Two figures are provided for each contaminant particle showing a low range with contaminant particle size ranging from 50 to 100 nm in radius to a high range between 100 and 500 nm in

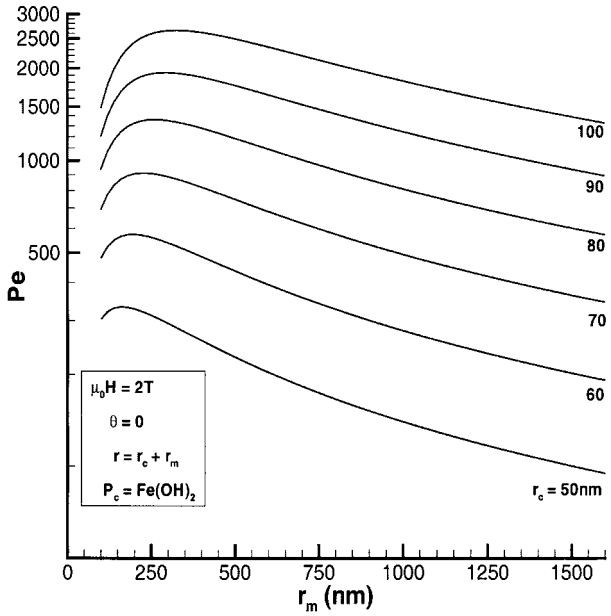

Figure 6. *Pe* as a function of r_m with different r_c (50–100 nm) for $P_c = Fe(OH)_2$ at r_{min}.

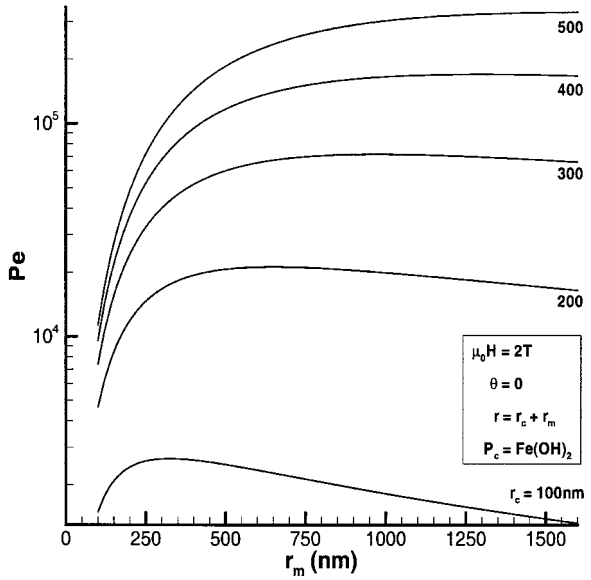

Figure 7. *Pe* as a function of r_m with different r_c (100–500 nm) for $P_c = Fe(OH)_2$ at r_{min}.

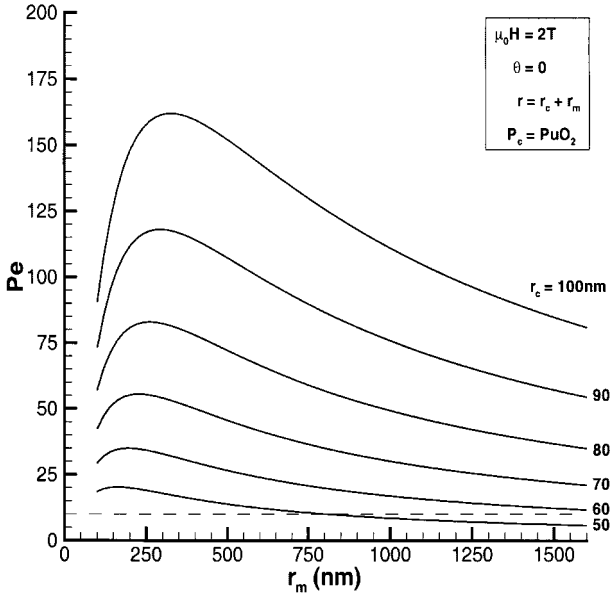

Figure 8. *Pe* as a function of r_m with different r_c (50–100 nm) for $P_c = PuO_2$ at r_{min}.

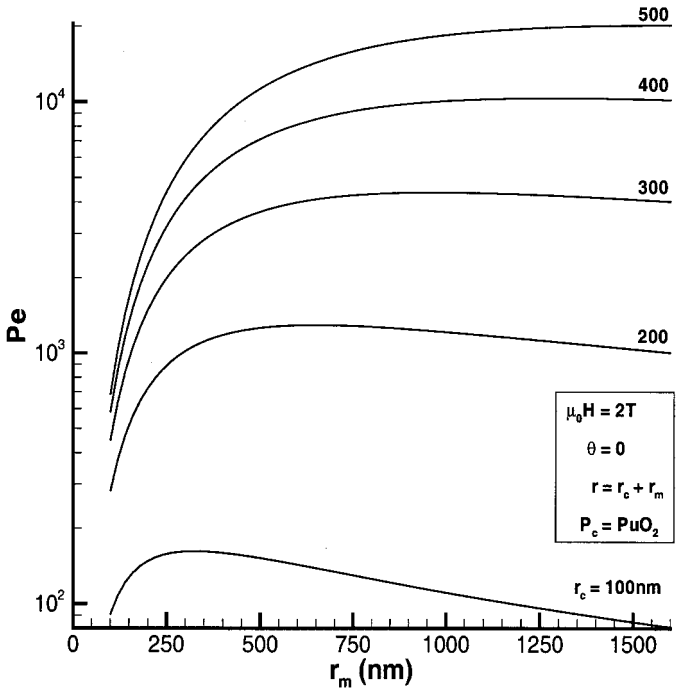

Figure 9. *Pe* as a function of r_m with different r_c (100–500 nm) for $P_c = PuO_2$ at r_{min}.

contaminant particle radius. Note that there are clearly peaks to the curves where this model predicts magnetic separation is maximized. These figures indicate that magnetic separator performance can be altered by the selection and use of matrix particles with different radii. However, it is important to note that particularly with larger particles ($r_c > 100$ nm), Peclet reaches a maximum and only slightly decreases with increasing matrix particle size. This implies that as matrix particle size increases above approximately 500 nm in radius, little improvement in magnetic separation efficiency is achieved.

Looking at the maxima of the curves in Figs. 6 and 8 reveals an interesting point. Taking the derivative of Eqs. (5) and (6) and setting it equal to zero yields the following:

$$\frac{dF_{m_r}}{d_{r_m}} = 0|_{\theta=0,r=r_m+r_c} = \frac{d}{d_{r_m}}\left[-\frac{8}{3}\pi r_c^3 \mu_0(\chi_c - \chi_m)M_I \times\left(\frac{r_m^3}{(r_m + r_c)^4}\right)\left(H + \frac{2r_m^3}{3(r_m + r_c)^3}\right)M_I\right] \quad (12)$$

$$\frac{\mathrm{d}}{\mathrm{d}_{r_\mathrm{m}}}=\left[\left(\frac{3r_\mathrm{m}^2}{(r_\mathrm{m}+r_\mathrm{c})^4}-\frac{4r_\mathrm{m}^3}{(r_\mathrm{m}+r_\mathrm{c})^5}\right)\left(H+\frac{2r_\mathrm{m}^3}{3(r_\mathrm{m}+r_\mathrm{c})^3}M_\mathrm{I}\right)+\frac{r_\mathrm{m}^3}{(r_\mathrm{m}+r_\mathrm{c})^4}M_\mathrm{I}\left(\frac{2r_\mathrm{m}^2}{(r_\mathrm{m}+r_\mathrm{c})^3}-\frac{2r_\mathrm{m}^3}{(r_\mathrm{m}+r_\mathrm{c})^4}\right)=0\right] \tag{13}$$

And making the substitution of Eq. (14) into Eq. (13) yields

$$\Psi=\frac{r_\mathrm{m}}{r_\mathrm{m}+r_\mathrm{c}} \tag{14}$$

$$(3-4\Psi)\left(H+\frac{2}{3}\Psi^3M_\mathrm{I}\right)+2M_\mathrm{I}(\Psi^3-\Psi^4)=0 \tag{15}$$

With the substitution of Eq. (16) and simplification results in

$$\omega=\frac{M_\mathrm{I}}{H}=\frac{\mu_0M_\mathrm{I}}{\mu_0H}=\frac{0.615}{2}=0.3075 \tag{16}$$

$$14\omega\Psi^4-12\omega\Psi^3+12\Psi-9=0 \tag{17}$$

Equation (17) has two roots and the positive one is 0.7648. Rearranging Eq. (14) yields

$$r_\mathrm{m}=\frac{\Psi}{1-\Psi}r_\mathrm{c}=\frac{0.7648}{1-0.7648}r_\mathrm{c}=3.252r_\mathrm{c} \tag{18}$$

which shows the maximum attractive force is independent of contaminant magnetic susceptibility and the optimum contaminant to matrix particle size is a constant.

Figure 10 shows the flow component in the system as represented by the particle Reynolds number. The drag force represents the shear that a contaminant particle would be subject to as it is magnetically held to a matrix particle. This shear will increase with increasing bulk fluid flow and limiting conditions of particle and matrix size, applied magnetic field strength, and flow are presented. The PuO_2 particle size varies from 50 to 500 nm in particle radius and the magnetic field intensity is varied from 2 to 10 T. A contaminant particle size limitation due to flow-induced drag can be seen by looking at a line $\vartheta=1$, i.e., $|\vec{F}_\mathrm{m}|=|\vec{F}_\mathrm{d}|$. To the left of this line, drag forces will cause the contaminant particle to be swept away from the matrix particle. The minimum particle size that can be retained in a magnetic separator under $Re_\mathrm{p}=1\times10^{-5}$ ($\nu\ll0.1\,\mathrm{m\,sec^{-1}}$) flow ranges from approximately 370 nm for an applied magnetic intensity of 2 T to approximately 170 nm for 10 T. In order for magnetic separation of smaller particles to occur, the flow rate would have to be decreased or the applied magnetic field intensity increased.

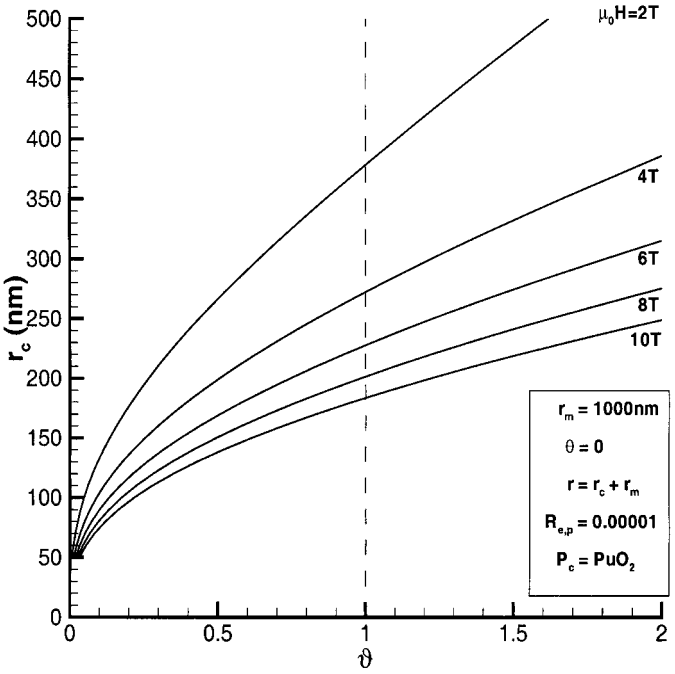

Figure 10. r_c as a function of ϑ with different $\mu_0 H$ for $P_c = PuO_2$ at r_{min}.

Figure 11 shows the results of varying the flow rate as shown by various particle Reynold's number values. Noting regions where $\vartheta > 1$, magnetic separation can be accomplished for 500 nm PuO_2 particles by a 1000-nm magnetite matrix element with flows corresponding to $Re_p < 1 \times 10^{-5}$. Since the drag force and particle Reynold's number are linear with velocity as shown in Eqs. (1) and (9), respectively, the curves are parallel. Recent work by Ebner et al.[43] discusses the ability of contaminant particles to be held within the boundary layer surrounding the magnetite particle. This will allow for increased flow while maintaining particle retention so the above discussion would be considered conservative.

CONCLUSIONS

This work effectively couples the magnetic force equations and hydrodynamic drag force equations to model a magnetic separator employing a spherical magnetite matrix element and spherical contaminant nanoparticles.

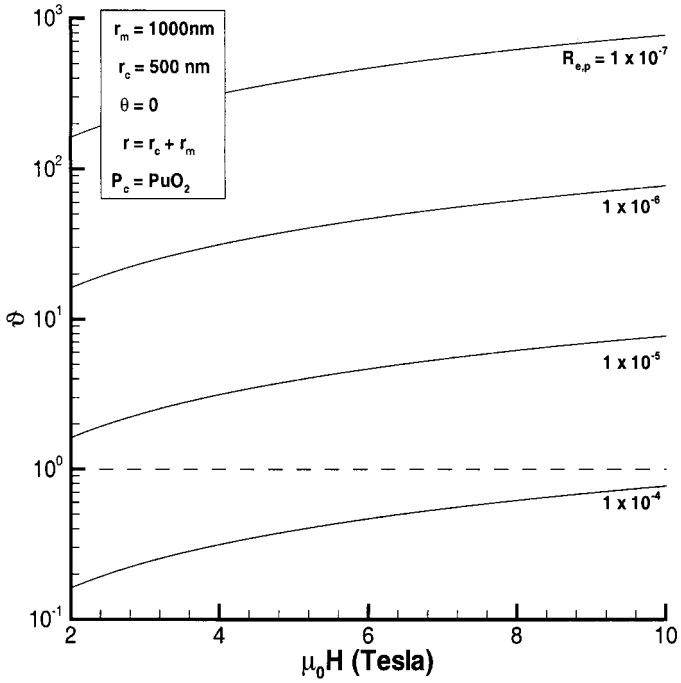

Figure 11. ϑ as a function of $\mu_0 H$ with different Re_p for $P_c = PuO_2$ at r_{min}.

The influence of particle size of both the magnetic matrix element and of the contaminant particle are presented indicating that sub-micron sized particles can be effectively separated magnetically in reasonable flow systems as their drag component is markedly small due to their radius, yet magnetic forces are sufficient to facilitate particle capture. Optimization of magnetic separators can be performed using this model. Actual treatment columns would be packed with many magnetite matrix particles and the mean probability of contaminant particle/matrix particle collision due to the tortuous path associated with a packed column would suggest a separation factor greater than depicted in this work could be expected. Ongoing work in the laboratory aims to quantify the capture efficiency of a magnetite-based magnetic separator for magnetically susceptible particles.

The theoretical model outputs presented in this work suggest process variables may be optimized to enhance magnetic separation. Extensive characterization of the contaminant feed stream and of the magnetic matrix material would be required to operate at peak efficiency. Since the model assumes single contaminant particle to single matrix particle interactions only,

packed column performance cannot be directly assumed to be as the model indicates. Matrix particle magnetic interactions and packed bed flow dynamics would have to be evaluated more fully. Magnetite may not be available in the small and discrete particle size ranges that this work indicates are necessary for superior performance.

APPENDIX A

Basic magnetic theory and nomenclature are provided here to support the model discussion. The essential magnetic concepts, variables, and nomenclature are presented where magnetic theory of spherical particles essentially reduces to near point charge electro-physics with materials that have sufficient free electrons to develop magnetic dipole moments.

Magnetic Theory

Magnetic field vectors[38] are expressed in either terms of magnetic induction B, in Tesla (T) or Weber per meter squared (Wb m^{-2}), or magnetic intensity H, in ampere-turns per meter, A-t m^{-1} or A m^{-1}. For paramagnetic and diamagnetic materials, the two field vectors are related by

$$\vec{B} = \mu_m \vec{H} \tag{A1}$$

with the magnetic permeability of the material, particle, or medium, μ_m, as the "proportionality constant," although μ_m is not constant for all materials, but changes as a ferromagnetic material approaches magnetic saturation. For magnetically susceptible material, Eq. (A1) is commonly assumed linear in the region of interest, namely prior to saturation. The permeability of free space (vacuum) has the value of $\mu_0 = 4\pi \times 10^{-7}$ Wb(A m)$^{-1}$ and it should be noted that for nonmagnetic materials, Eq. (A1) is linear. When a magnetic field passes through a material, or particle, it acquires an induced magnetization M_I given by

$$\vec{M}_I = \chi_m \vec{H} \tag{A2}$$

Diamagnetic particles have negative susceptibilities with values on the order of -1×10^{-5} to -1×10^{-7} (e.g., $\chi_{lead} = -2.3 \times 10^{-5}$, $\chi_{copper} = -1 \times 10^{-7}$) and in an induced field, cancel part of the magnetic field intensity. Paramagnetic particles have positive susceptibilities on the order of 1×10^{-5} to 1×10^{-3} (e.g., $\chi_{aluminum} = 1.05 \times 10^{-5}$, $\chi_{uranium} = 3.95 \times 10^{-4}$) and induced magnetization augments the magnetic flux density. Ferromagnetic materials (e.g., iron, nickel, and cobalt) generally do not have constant susceptibilities, and permeability is

used to define these materials (e.g., $\mu_{\text{ferromagnetics}} \geq 4\pi \times 10^{-4}\,\text{Wb(A m)}^{-1}$ and by comparison $\mu_0 \approx \mu_{\text{air}} \approx \mu_{\text{copper}}$).[41,42,44–46]

Whenever a magnetic particle is placed in a magnetic field, the magnetic induction B is given by

$$\vec{B} = \mu_0(\vec{H} + \vec{M}_\text{I}) \tag{A3}$$

whereby it equals the permeability of free space times the sum of the applied magnetic intensity and the induced magnetization. Equations (A1)–(A3) can be combined to show

$$\mu_{\text{p,m}} = \mu_0(1 + \chi_\text{m}) \tag{A4}$$

which is useful in relating magnetic permeability and susceptibility.

The magnetic force on a small weakly magnetic particle placed in an external magnetic field is given by Svoboda[34] as

$$\vec{F_\text{m}} = \frac{2}{3}\pi r_\text{p}^3 \chi_\text{m} \vec{H} \nabla \vec{B} = \frac{2}{3}\pi r_\text{p}^3 \mu_0 \chi_\text{m} \nabla(H^2) \tag{A5}$$

A dimensional analysis of Eq. (A5), after substituting Eq. (A1), yields

$$F_\text{m} = \text{m}^3 \frac{\frac{\text{Wb}}{\text{m}^2}}{\frac{\text{Wb}}{\text{A m}}} \frac{\text{Wb}}{\text{m}^3} = \frac{\text{A}}{\text{m}}\text{Wb} = \text{H Wb} = \frac{\text{A}}{\text{m}}\text{V sec} = \frac{\frac{\text{C}}{\text{sec}}}{\text{m C}}\text{J sec} = \frac{\text{J}}{\text{m}}$$

$$= \frac{\text{N m}}{\text{m}} = \text{N} \tag{A6}$$

where V is volts, sec is seconds, C is Coulombs, J is Joules, and N is Newtons, the standard unit of force.

Equation (A2) can be modified to account for the net induced magnetism over the medium it is in by

$$\vec{M}_\text{I} = \frac{\mu_{\text{p,m}} - \mu_\text{m}}{\mu_\text{m}} \vec{H} \tag{A7}$$

with μ_m defined as the permeability of the medium, in this case, water.

Radial and angular components of the magnetic force in spherical coordinates derived from the Biot–Savart law are

$$H_\text{r} = \frac{\frac{4}{3}\pi r_\text{m}^3 M_\text{I} \cos\theta}{2\pi r^3} = \frac{2}{3}\left(\frac{r_\text{m}}{r}\right)^3 M_\text{I} \cos\theta \tag{A8}$$

$$H_0 = \frac{\frac{4}{3}\pi r_\text{m}^3 M_\text{I} \sin\theta}{4\pi r^3} = \frac{1}{3}\left(\frac{r_\text{m}}{r}\right)^3 M_\text{I} \sin\theta \tag{A9}$$

and substituting Eq. (A7) into Eq. (A5) and then adding in Eqs. (A8) and (A9) yield Eqs. (5) and (6) of the main text.

ACKNOWLEDGMENTS

Drs. D. Gombert and M. Harrup of the Idaho National Engineering & Environmental Laboratory (INEEL) provided helpful comments and criticisms. The work described in this paper was supported by the United States Department of Energy and the INEEL under contract DEAC07-99ID13727.

REFERENCES

1. Watson, J.H.P. Status of Superconducting Magnetic Separation in the Minerals Industry. Miner. Eng. **1994**, *7* (5/6), 737–746.
2. Kolm, H.; Oberteuffer, J.; Kelland, D. High-Gradient Magnetic Separation. Sci. Am. **1975**, *233* (5), 46–54.
3. Worl, L.A.; Hill, D.D.; Padilla, D.D.; Prenger, F.C. Magnetic Separation for Nuclear Material Detection and Surveillance. Abstr. Pap. Am. Chem. Soc. **1998**, *216* (67-I&EC), Part 1.
4. Ginn, M.W. High Gradient Wet Magnetic Separation, Brightening the Future of Industry, Presented at the SME Annual Meeting, Denver, CO, March 1–3, 1999.
5. Gurevitz, D. Method and Apparatus for Processing Waste Water, United States Patent 5,759,407, June 2, 1998.
6. Harusuke, N. Water Purifier Having a Magnetic Field Generation Device, United States Patent 5,628,900, May 13, 1997.
7. Stadmuller, A. Magnetic Separators, United States Patent 5,759,391, June 2, 1998.
8. Kelland, D.R. Magnetic Separation of Nanoparticles. IEEE Trans. Magn. **1998**, *34* (4), 2123–2125.
9. Dixit, S.G. Kinetics of Particle Deposition on Filaments in High Gradient Magnetic Separation. Trans. Indian Inst. Metall. **1997**, *50* (5).
10. Gillet, G.; Diot, F. Technology of Superconducting Magnetic Separation in Mineral and Environmental Processing. Miner. Metall. Process. **1999**, *16* (3).
11. Watson, J.H.P.; Beharrell, P.A. Magnetic Separation Using a Switchable System of Permanent Magnets. J. Appl. Phys. **1997**, *81* (8), 4259–4262.
12. Avens, L.R.; Gallegos, U.F.; McFarlan, J.T. Magnetic Separation as a Plutonium Residue Enrichment Process. Sep. Sci. Technol. **1990**, *25* (13–15), 1967–1979.
13. Avens, L.R.; Worl, L.A.; Deaguero, K.J.; Prenger, F.C.; Stewart, W.F.; Hill, D.D.; Tolt, T.L. Environmental Remediation Using Magnetic Separation. Abstr. Pap. Am. Chem. Soc. **1993**, *205* (135-IEC), Part 1.

14. Padilla, D.D.; Schake, A.R.; Avens, L.R.; Worl, L.A. Magnetic Separation to Remove Actinides from Soils. Abstr. Pap. Am. Chem. Soc. **1994**, *208* (13-TECH), Part 1.
15. Padilla, D.D.; Worl, L.A.; Schake, A.R.; Avens, L.R.; Romero, D. Magnetic Separation to Remove Actinides from Soil. Abstr. Pap. Am. Chem. Soc. **1995**, *209* (8-TECH), Part 1.
16. Padilla, D.D.; Worl, L.A.; Hill, D.D.; Prenger, F.C.; Tolt, T.L. Magnetic Separation for Treatment of Caustic Waste. Abstr. Pap. Am. Chem. Soc. **1996**, *211* (34-TECH), Part 1.
17. Kochen, R.L.; Navratil, J.D. Removal of Radioactive Materials and Heavy Metals from Water Using Magnetic Resin, United States Patent 5,595,666, January 21, 1997.
18. Ebner, A.D.; Ritter, J.A.; Nuñez, L. High Gradient Magnetic Separation for the Treatment of High Level Radioactive Wastes. Sep. Sci. Technol. **1999**, *34* (6&7), 1333–1350.
19. Ebner, A.D.; Ritter, J.A.; Ploehn, H.J.; Kochen, R.L.; Navratil, J.D. New Magnetic Field-Enhanced Process for the Treatment of Aqueous Wastes. Sep. Sci. Technol. **1999**, *34* (6&7), 1277–1300.
20. Schake, A.R.; Avens, L.R.; Worl, L.A.; Deaguero, K.J.; Padilla, D.D.; Prenger, F.C.; Stewart, W.F.; Hill, D.D.; Tolt, T.L. Magnetic Separation for Environmental Remediation. Abstr. Pap. Am. Chem. Soc. **1994**, *207* (213-IEC), Part 1.
21. Rikers, R.A.; Rem, P.; Dalmijn, W.L. Improved Method for Prediction of Heavy Metal Recoveries from Soil Using High Intensity Magnetic Separation (HIMS). Int. J. Miner. Process. **1998**, *54*, 165–182.
22. Padilla, D.D.; Worl, L.A.; Devilin, D.; Prenger, F.C.; Hill, D.D. High-Performance Magnetic Separation for Actinide Particle Collection. Abstr. Pap. Am. Chem. Soc. **1999**, *218* (28-TECH), Part 1.
23. Sheerer, T.J.; Parker, M.R.; Friedlaender, F.J.; Birss, R.R. Theory of Capture of Weakly Magnetic Particles in Random Matrices in the Longitudinal Configuration in HGMS. IEEE Trans. Magn. **1981**, *MAG-17* (6), 2807–2809.
24. Blums, E.; Mezulis, A.; Maiorov, M.; Kronkalns, G. Thermal Diffusion of Magnetic Nanoparticles in Ferrocolloids: Experiments on Particle Separation in Vertical Columns. J. Magn. Magn. Mater. **1997**, *169*, 220–228.
25. Abbasov, T.; Herdem, S.; Köksal, M. Performance of High Gradient Magnetic Filters with Granular Matrix. Sep. Sci. Technol. **1999**, *34* (2), 263–276.
26. Natenapit, M.; Sanglek, W. Capture Radius of Magnetic Particles in Random Cylindrical Matrices in High Gradient Magnetic Separation. J. Appl. Phys. **1999**, *85* (2), 660–664.

27. Tsouris, C.; Scott, T.C. Flocculation of Paramagnetic Particles in a Magnetic Field. J. Colloid Interface Sci. **1995**, *171*, 319–330.
28. Tsouris, C.; Scott, T.C.; Harris, M.T. Para- and Dia-magnetic Particle Flocculation in a Magnetic Field. Sep. Sci. Technol. **1995**, *30* (7–9), 1407–1419.
29. Tsouris, C.; Yiacoumi, S. Particle Flocculation and Filtration by High-Gradient Magnetic Fields. Sep. Sci. Technol. **1997**, *32* (1–4), 599–616.
30. Yiacoumi, S.; Rountree, D.A.; Tsouris, C. Mechanism of Particle Flocculation by Magnetic Seeding. J. Colloid Interface Sci. **1996**, *184*, 477–488.
31. Ying, T.-Y.; Chin, C.J.; Lu, S.-C.; Yiacoumi, S.; Chattin, M.R.; Spurrier, M.A.; DePaoli, D.W.; Tsouris, C. Magnetic-Seeding Filtration. Sep. Sci. Technol. **1999**, *34* (6&7), 1371–1392.
32. Ying, T.-Y.; Yiacoumi, S.; Tsouris, C. High-Gradient Magnetically Seeded Filtration. Chem. Eng. Sci. **1999**, *55* (2000), 1101–1113.
33. Friedlaender, F.J.; Gerber, R.; Kurz, W.; Birss, R.R. Particle Motion Near and Capture on Single Spheres in HGMS. IEEE Trans. Magn. **1981**, *MAG-17* (6), 2801–2803.
34. Svoboda, J. *Magnetic Methods for the Treatment of Minerals*; Elsevier: Amsterdam, 1987.
35. Abbasov, T.; Ceylan, K. Estimation of Optimum Fluid Velocity in High Gradient Magnetic Filtration. Sep. Sci. Technol. **1998**, *33* (7), 975–989.
36. Zhang, X.; Basaran, O.A.; Wham, R.M. Theoretical Prediction of Electric Field-Enhanced Coalescence of Spherical Drops. Am. Inst. Chem. Eng. J. **1995**, *41* (7), 1629–1639.
37. Davis, R.H. Hydrodynamic Diffusion of Suspended Particles: A Symposium. J. Fluid Mech. **1996**, *130*, 325–335.
38. Perry, R.H., Ed. *Perry's Chemical Engineer's Handbook*, 6th Ed.; McGraw-Hill: New York, 1984.
39. Ebner, A.D.; Ritter, J.A.; Ploehn, H.J. Feasibility and Limitations of Nanolevel High Gradient Magnetic Separation. Sep. Purif. Technol. **1997**, *11*, 199–210.
40. De Nevers, N. *Fluid Mechanics*; Addison-Wesley Publishing Company, Inc.: Reading, PA, 1977.
41. Bozorth, R.M. *Ferromagnetism*; IEEE Press: Piscataway, NJ, 1978.
42. Reitz, J.R.; Milford, F.J.; Christy, R.W. *Foundations of Electromagnetic Theory*; Addison-Wesley Publishing Company: Reading, MA, 1993.
43. Ebner, A.D.; Ritter, J.A.; Ploehn, H.J. Magnetic Hetero-flocculation of Paramagnetic Colloidal Particles. J. Colloid Interface Sci. **2000**, *225*, 39–46.

44. Scott, W.T. *The Physics of Electricity and Magnetism*; John Wiley & Sons, Inc.: New York, 1959.
45. Carlin, R.L.; van Duyneveldt, A.J. *Magnetic Properties of Transition Metal Compounds*; Springer-Verlag: New York, 1977.
46. Lide, D.R. Ed.; *CRC Handbook of Chemistry and Physics*, 74th Ed.; CRC Press: Boca Raton, 1993.

Received September 2001
Revised January 2002